

In-plane magneto-plasmons in grating gated double quantum well field effect transistors.

X. G. Peralta, S. J. Allen

Center for Terahertz Science and Technology and iQUEST,
University of California, Santa Barbara, California 93106, U. S. A.

M. C. Wanke, J. A. Simmons, M. P. Lilly, J. L. Reno

Sandia National Laboratories, Albuquerque, New Mexico 87185, U. S. A.

P. J. Burke, J. P. Eisenstein

Department of Physics, California Institute of Technology,
Pasadena, California 91125, U. S. A.

Abstract. Coupled double quantum well field-effect transistors with a grating gate exhibit a terahertz (~600 GHz) photoconductive response that resonates with standing two dimensional plasma oscillations under the gate and may be the basis for developing a fast, tunable terahertz detector. The application of a precisely aligned in-plane magnetic field produces no detectable change in the device DC conductance but produces a dramatic inversion, growth of the terahertz photoconductive response and frequency shift of the standing plasmon resonances. The frequency shift can be described by a significant mass increase produced by the in-plane field. The mass increase is substantially larger than that calculated from a single well and we presume that a proper treatment of the coupled double quantum well may resolve this discrepancy.

1. Introduction

High mobility double quantum well heterostructures have been important for the study of correlated electron states in two dimensional electron systems [1, 2] and are potentially important for novel field-effect transistors that add functionality by controlling electron transfer between the quantum wells [3]. Interwell transfer can also be promoted by terahertz photon assisted tunnelling [4], opening the possibility of fast, voltage tunable terahertz detectors. To this end we have explored the terahertz response of double well field-effect transistors with large area channels gated with a grating gate. We demonstrate a fast, tunable terahertz photoconductive response and correlate the observed resonances with standing plasma waves under the metallic part of the grating gate [5, 6].

Collective excitations in the presence of in-plane magnetic fields have received limited attention over the years [7]. We note the experiments by Batke et al. on a single two dimensional electron gas (2DEG) and theoretical treatments of double quantum wells [8-10].

The ability to probe plasmon modes by means of terahertz photoconductivity measurements enables us to explore the effect of in-plane magnetic fields on the collective excitations of these double quantum well systems. We observed a dramatic inversion, growth of the terahertz photoconductive response and frequency shift of the standing plasmon resonances. The dependence on electron density indicates that the frequency shift is caused by a change in mass. A model based on a single quantum well predicts a change in mass ~ 3 times smaller than that observed. We speculate that the correct treatment of the coupled double quantum wells will lead to a mass increase similar to that seen in the experiment but this has not been confirmed at this time.

2. Experimental details

2.1. Sample structure

The field effect devices are fabricated from modulation doped GaAs/AlGaAs double quantum well heterostructures grown on a semi-insulating GaAs substrate by molecular beam epitaxy. Both quantum wells are 200 Å wide and are separated by a 70 Å barrier. The nominal electron densities in the quantum wells are $n_{\text{upper}}=1.7\times 10^{11}$ cm⁻² and $n_{\text{lower}}=2.57\times 10^{11}$ cm⁻²: the 4.2 K mobility is $\sim 1.7\times 10^6$ cm²/V s. A 2×2 mm mesa is defined by wet chemical etching and the source and drain ohmic contacts to both quantum wells are formed by evaporating and annealing NiAuGe over the edge and side of the mesa. A 700 Å thick TiAu grating gate (with no metallization between the grating fingers) is evaporated with the lines of the grating parallel to the ohmic contacts, perpendicular to the current flow. Grating periods of 4 and 8 μm were explored where half the period is metal. The grating modulates the electron density in the quantum wells by acting as a gate when a voltage is applied, selects the wavevectors of the excited plasmon and, coincidentally, produces both normal and transverse terahertz electric fields.

2.2. Measurement technique

In order to measure the terahertz photoresponse, the samples are wire bonded and mounted onto a fiberglass chip carrier that is placed inside a variable temperature cryostat equipped with a 12 Tesla superconducting magnet. Radiation is focused onto the sample with an off-axis parabolic mirror. We apply a constant source-drain current of 100 μA and study the photoconductive response of the double quantum wells as a function of gate voltage, terahertz frequency, temperature and in-plane magnetic field.

The radiation sources are the free-electron lasers at University of California, Santa Barbara, which cover a frequency range between 120 GHz and 4.8 THz. The terahertz radiation is polarized perpendicular to the lines of the grating gate. Results were obtained in the low power limit by assuring that the response was a linear function of incident power. It was also ascertained that the response was linear with respect to source-drain current (it is photoconductive, not photovoltaic) in the region studied. Part of the terahertz radiation is split off by means of a mylar beamsplitter and is focused, using an off-axis parabolic mirror, onto a fast pyroelectric detector that acts as a reference. In order to account for pulse-to-pulse variations in the output power of the free-electron laser and to be able to compare results for different frequencies, the photoconductive signal was normalized by dividing it by the signal from the reference pyroelectric detector. All the data presented has been normalized in this manner.

3. Plasmon resonances

3.1. Experimental results

Figure 1 shows the terahertz photoresponse as a function of gate voltage at three frequencies and a temperature of 25 K for two different grating periods: 4 μm (1a) and 8 μm (1b). We observe that both grating periods show a resonant response that moves to lower gate voltage, higher electron density, as we increase the frequency of the incident radiation (follow arrows). This is typical plasmon behavior, which invariably exhibit an increasing frequency with increasing electron density [11]. Note that the larger the period, the greater the number of resonances in a voltage interval.

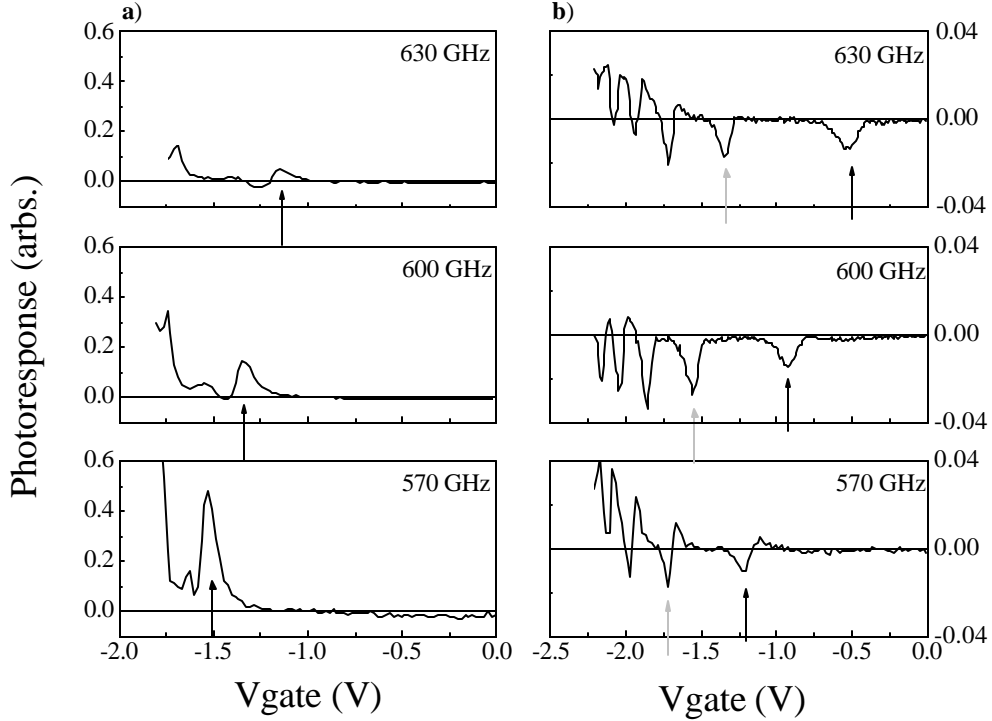


Figure 1. Terahertz photoresponse as a function of gate voltage at three frequencies for two grating periods: **a)** 4 μm and **b)** 8 μm . Frequencies **top to bottom:** 630, 600 and 570 GHz. $T=25$ K. Arrows indicate resonance positions.

While the plasmon dispersion relations of double quantum wells and single quantum wells close to a uniform metal gate are known, there is no simple model for plasmons under a discontinuous metal grating [12]. In order to confirm that the resonances are caused by plasmon modes underneath the metal grating and get a better understanding for the dependence on grating size, we constructed a model that captures the essential physics.

3.2. Modeling

We modeled the collective response of the composite structure by treating the double quantum well as a single quantum well, ignoring the effect of fringing fields on the ungated regions and using an equivalent circuit. In the ungated region we combine the electron sheet densities of the two quantum wells into one ($n_{\text{effective}} = n_{\text{upper}} + n_{\text{lower}}$) and keep it fixed. We also include a capacitive term that takes into account the presence of the periodic grating.

The region underneath the grating metal is modeled as a transmission line with a variable density 2DEG (ranging from $n_{\text{effective}}$ to zero) [13]. The total impedance is the series combination (sum) of the impedances of the gated and ungated regions. Using the equivalent circuit we calculate the ratio of the absorbed power to the incident power (normalized absorption) as a function of the electron density under the the grating metallization, which is controlled by the gate voltage. We then find the resonances of the normalized absorption and compare them to the experimental results as presented in reference [5]. The model captures the dependence on frequency, period and density but fails to provide us with an accurate dispersion relation. It enables us to identify the resonances with the optic plasmons of the double quantum well system with an odd number of half wavelengths under a metallic element of the grating gate. Armed with this assignment of the resonances we use a more accurate description of the dispersion relation provided by a single 2DEG with a distant uniform metal gate and find a good agreement with the observations.

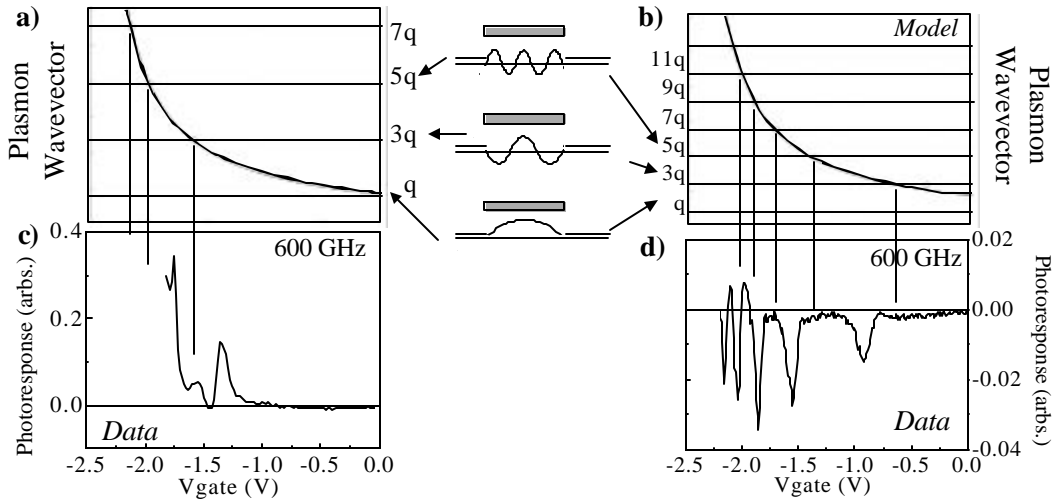


Figure 2. Comparison between modeling results and experimental data at 600 GHz. **Top:** Plasmon wavevector of a 2DEG inside a semiconductor with a distant metal gate as a function of gate voltage for the **a)** 4 μm and **b)** 8 μm grating periods respectively. Horizontal lines correspond to odd integer number of plasmon $\frac{1}{2}$ wavelengths. Vertical lines are located at the intersections. **Bottom:** Photoreponse as a function of gate voltage for the **c)** 4 μm and **d)** 8 μm grating period samples respectively – experimental results. **Middle column:** schematic representation of current density distribution under the metal gate at resonance.

The upper plots in figure 2 show the plasmon wavevector of a 2DEG embedded in a semiconductor with a distant metal gate at 600 GHz as a function of gate voltage for the two different grating sizes. (At these wave vectors the metallization is not important.) The horizontal lines are located at odd integer multiples of half the wavelength defined by the grating via the wavevector $q = 2p/a$, where a is the grating period. The point at which the horizontal lines intersect the plasmon wavevector correspond to having an odd integer number of plasmon $\frac{1}{2}$ wavelengths underneath the metal gate element, a standing plasmon mode. Although they do not exactly match the resonant peak positions, we observe that their spacing is relatively close to that of the resonant peaks in the data (figures 2c and 2d).

Relating figures 2a and 2b to the data we can roughly say that the first resonance, from right to left, corresponds to the third harmonic with wavevector $3q = 3 \times (2p/a)$ for both grating periods. The middle column is a schematic representation of the current density distribution under the metal gate for the corresponding resonant modes.

A more rigorous and complete treatment of the problem has recently been carried out by Popov and coworkers and shared with us [14]. Space does not permit us to display their results here but they largely support the interpretation described above. Their model has the potential of a complete description of the normal modes of the standing plasmon excitations and other important features like the sign reversal in the photoconductive response.

The fact that one observes a larger number of resonances with the 8 μm period grating than with the 4 μm arises because one can fit a larger number of standing plasmon modes underneath a larger grating metallization.

4. In-plane magneto-plasmons

In order to explore the role of the double quantum wells, terahertz photoconductivity experiments were performed with a magnetic field in the plane of the 2DEGs, parallel to the grating. It is known that in-plane magnetic fields change the coupling and the tunneling between the wells by producing a relative shift of the in-plane single particle dispersion relations.

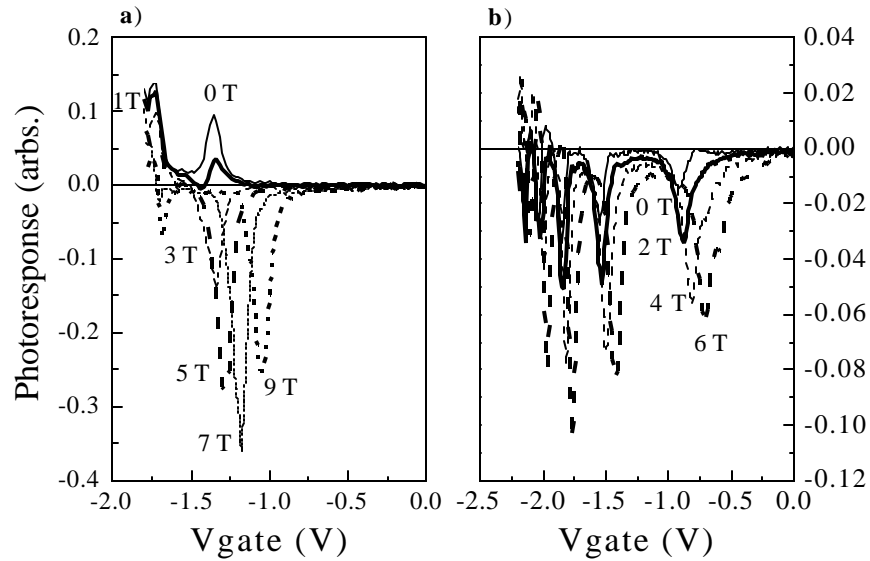


Figure 3. In-plane magnetic field dependence of the terahertz photoconductivity at 600 GHz for two grating periods: **a)** 4 μm and **b)** 8 μm . $T=25$ K.

The application of a precisely aligned in-plane magnetic field produces no detectable change in the device DC conductance. Indeed, alignment is achieved by nulling the effect of a perpendicular component. Figure 3 shows the in-plane magnetic field dependence of the terahertz photoconductivity at 600 GHz and $T=25$ K for two grating periods: 4 μm (3a) and 8 μm (3b). For both grating periods, the resonance position moves to lower gate voltages as we increase the magnitude of the in-plane magnetic field. For the 4 μm grating period, the in-plane magnetic field also causes an inversion of the photoconductive signal and an increase in the negative going signal. At higher magnetic fields, due to the shift of the resonant response to lower gate voltages, one can resolve another resonance at higher negative gate voltages.

For the 8 μm grating period applying an in-plane magnetic field does not cause an inversion of the photoconductive plasma resonant response as it starts out negative, but it does cause an increase as well as a shift in the resonant gate voltage position.

4.1. Analysis

The resonances are caused by standing plasmons modes underneath the metallic part of the grating. However complex the dispersion relation, the frequencies will be *largely* determined by the ratio of the electron density and mass. An increase in density at resonance can signal an increase in mass, if the fractional increase in density at resonance is independent of density.

Inspection of figure 4 shows this to be the case. Figure 4a is a plot of the resonant peak position as a function of magnetic field squared for the 8 μm grating period. The change in gate voltage for resonance is largest at voltages corresponding to larger density (figure 4a). In figure 4b we gather all the data for each of the spatial resonances, overtones, and plot the voltage difference caused by the in-plane magnetic field ($V_B - V_0$) divided by the $B = 0$ Tesla voltage at resonance referenced to the threshold voltage ($V_0 - V_{\text{th}}$) where threshold is the voltage at which both wells are fully depleted. This effectively measures the fractional change in mass under the metallization. When plotted in this manner, all the data fall on a straight line; the fractional change is independent of density. The slope is proportional to the change in the effective mass due to the in-plane magnetic field. If we fit the data with a straight line, we obtain a 30% increase in the effective mass at 9 Tesla, black line in figure 4b). Doing the same analysis with the 4 μm grating period data yields an increase of 33%.

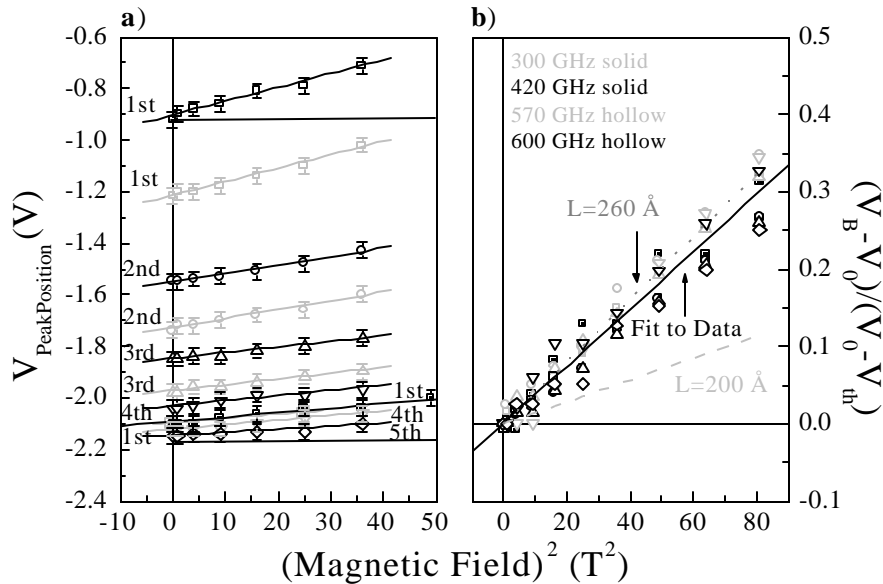


Figure 4. Analysis to extract the effective mass change due to the in-plane magnetic field. **a)** Peak position as a function of magnetic field squared for different harmonics (symbols) and frequencies (filling and color). **b)** Relative change in peak position as a function of magnetic field square. The legend is the same for both plots.

If we calculate the first and second order corrections to the energy levels of a confined state in a single quantum well due to an in-plane magnetic field, we find that there is a correction to the effective mass given as

$$m^*(B) = m^*(0) \left[1 - \left(\frac{L}{l_B} \right)^4 \frac{1}{\mathbf{p}^6} \left(\frac{4}{3} \right)^5 \right]^{-1}, \quad l_B = \sqrt{\hbar/eB} \quad (1)$$

where m^* is the mass of the electron, L is the well width, l_B is the magnetic length and B is the magnetic field strength. This means that the reciprocal of the effective mass decreases quadratically with the in-plane magnetic field strength [8]. The plasmon resonance will be depressed accordingly and the voltage or density for resonance increased. From this simple calculation one would expect there to be an 13% increase in the effective mass going from 0 to 9 Tesla for a 200 Å well. Going back to figure 4b, from the fit to the data we know that in a 9 Tesla field the mass increases by ~30%. For comparison, we have included the results obtained from equation (1) for a 200 Å (light gray dashed line) and a 260 Å (gray dotted line) well. A 260 Å wide quantum well may simulate the behavior of the coupled double quantum well but this requires confirmation.

5. Conclusions

We have observed a resonant photoresponse in coupled double quantum well field effect transistors corresponding to the excitation of standing plasma waves under the metallic part of a grating gate. The resonance can be tuned by means of a gate or by changing the period of the grating. While we understand that the tunable resonance is caused by the composite plasma oscillations, the mechanism that gives rise to the change in conductance at resonance is not understood. Particularly striking is the sign reversal between the 4 and 8 μm devices and the sign reversal induced by the magnetic field in the 4 μm device.

The results suggest that the resonant photoresponse is conditioned on the presence of a double quantum well channel. Experiments were carried out on a similar device with a single quantum well [5, 6]. No resonant behaviour was observed but the mobility was sufficiently low that a direct comparison cannot be made. A high mobility single quantum well device needs to be investigated to support this conclusion.

In-plane magnetic fields alter the resonance condition by increasing the electron effective mass. We find a 34% increase in the effective mass at 9 Tesla whereas a single quantum well is expected to produce a 13% increase. This difference might be due to the fact that we really have a double quantum well system; one needs to include the presence of both wells and their coupling in the calculation of the corrections to the energy levels in order to obtain a more accurate estimate of the change in effective mass.

From the data presented we can see that grating gated double quantum well field effect transistors can be used as a tunable detector [15]. The response time has been measured to be no slower than 700 ns. It is a low impedance device and further measurements and device optimization may open the possibility of using the device as a heterodyne detector with intermediate frequency electronics integrated on the same chip.

Acknowledgments

The authors would like to thank D. Enyeart and G. Ramian at the Center for Terahertz Science and Technology and W. Baca at Sandia National Laboratories. This work was supported by the ONR MFEL program, the DARPA/ONR THz Technology, Sensing and Satellite Communications Program and the ARO, Science and Technology of Nano/Molecular Electronics: Theory, Simulation, and Experimental Characterization. Sandia

is a multiprogram laboratory operated by Sandia Corporation, a Lockheed Martin Company, for the United States Department of Energy under Contract DE-AC04-94AL85000.

References

- [1] J. P. Eisenstein, L. N. Pfeiffer and K. W. West, *Appl. Phys. Lett.* vol. 58, 1497 (1991).
- [2] I. B. Spielman, J. P. Eisenstein, L. N. Pfeiffer, K. W. West, *Phys. Rev. Lett.* vol. 84, 5808 (2000).
- [3] J. A. Simmons, M. A. Blount, J. S. Moon, S. K. Lyo, W. E. Baca and M. J. Hafich, *J. Appl. Phys.* vol. 84, 5626 (1998); J. S. Moon, J. A. Simmons, M. A. Blount, W. E. Baca, J. L. Reno and M. J. Hafich, *Elect. Lett.* vol. 34, 921 (1998).
- [4] H. Drexler, J. S. Scott, S. J. Allen, K. L. Campman, and A. C. Gossard, *Appl. Phys. Lett.* vol. 67, 2816 (1995).
- [5] X. G. Peralta, S. J. Allen, M. C. Wanke, N. E. Harff, J. A. Simmons, M. P. Lilly, J. L. Reno, P. J. Burke, J. P. Eisenstein, *Appl. Phys. Lett.* *in press*.
- [6] X. G. Peralta, S. J. Allen, W. Knap, Y. Deng, M. S. Shur, M. C. Wanke, N. E. Harff, J. A. Simmons, M. P. Lilly, J. L. Reno, P. J. Burke, J. P. Eisenstein, *Proceedings of Workshop on Frontiers of Electronics, January 2002, St. Croix, US V. I., International Journal of High Speed Electronics and Systems, in press.*
- [7] S.-J. Cheng and R. R. Gerhardts, *Phys. Rev. B* vol. 65, 085307 (2002) and references therein.
- [8] E. Batke and C. W. Tu, *Phys. Rev. B* vol. 34, 3027 (1986).
- [9] G. R. Aizin and G. Gumbs, *Phys. Rev. B* vol. 54, 2049 (1996).
- [10] X.-H. Liu and X.-H. Wang, *Phys. Rev. B* vol. 64, 195322 (2001).
- [11] S. Das Sarma and A. Madhukar, *Phys. Rev. B* vol. 23, 805 (1981).
- [12] C. D. Ager, R. J. Wilkinson and H. P. Hughes, *J. Appl. Phys.* vol. 71, 1322 (1992).
- [13] P. J. Burke, I. B. Spielman, J. P. Eisenstein, L. N. Pfeiffer and K. W. West, *Appl. Phys. Lett.* 76, 745 (2000).
- [14] V. V. Popov, N. J. M. Horing, O. V. Polischuk, T. V. Teperik and G. M. Tsymbalov, in preparation.
- [15] X. G. Peralta, S. J. Allen, M. C. Wanke, N. E. Harff, J. A. Simmons, M. P. Lilly, J. L. Reno, P. J. Burke and J. P. Eisenstein, *Proceedings of Far-IR, Sub-mm & mm Detector Technology Workshop, April 2002, Monterey, CA, in press.*